Biomacromolecules

pubs.acs.org/Biomac

Article

Peptide-Based Polyion Complex Vesicles That Deliver Enzymes into Intact Plants To Provide Antibiotic Resistance without Genetic Modification

Seiya Fujita, Yoko Motoda, Takanori Kigawa, Kousuke Tsuchiya,* and Keiji Numata*

Cite This: *Biomacromolecules* 2021, 22, 1080−1090

Read Online

ACCESS | Metrics & More | Article Recommendations | Supporting Information

ABSTRACT: Direct delivery of enzymes into intact plants using cell-penetrating peptides (CPPs) is an attractive approach for modifying plant functions without genetic modification. However, by conventional methods, it is difficult to maintain the enzyme activity for a long time because of proteolysis of the enzymes under physiological conditions. Here, we developed a novel enzyme delivery system using polyion complex vesicles (PICsomes) to protect the enzyme from proteases. We created PICsome-bearing reactive groups at the surface by mixing an anionic block copolymer, alkyne-TEG-P(Lys-COOH), and a cationic peptide, P(Lys). The PICsome encapsulated neomycin phosphotransferase II (NPTII), a kanamycin resistance enzyme, and protected NPTII from proteases in vitro. A CPP-modified PICsome delivered NPTII into the root hair cells of *Arabidopsis thaliana* seedlings and provided kanamycin resistance in the seedlings that lasted for 7 days. Thus, the PICsome-mediated enzyme delivery system is a promising method for imparting long-term transient traits to plants without genetic modification.

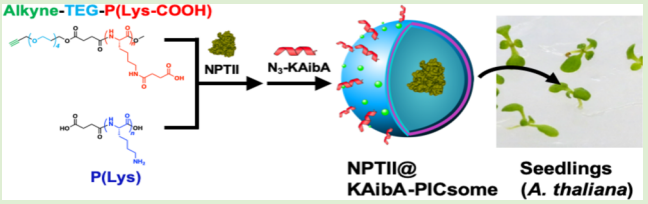

INTRODUCTION

Genetic engineering techniques for plants have been developed to impart resistance to environmental stresses,[1−3] including heat, drought, high salinity, and pesticides,[4,5] to improve crop productivity. Genetic modification of plants has been carried out by the delivery of exogenous DNA, encoding the desired trait to the plant genome by methods such as agrobacterium-mediated transformation, particle bombardment, poly(ethylene glycol) (PEG)-mediated transformation, and peptide fusion.[6,7] However, the genetic modification methods raise concerns about contamination of ecosystems due to inheritance between generations and horizontal transfer of the recombinant gene.[8] The resulting genetically modified plants are limited to a range of environments. Therefore, there is a demand for a technique to modify the traits of plants without genetic transformation.

The direct introduction of proteins for trait addition to plants has been studied as an alternative method to gene recombination.[9,10] One of these methods is conjugation of a target protein with cell-penetrating peptides (CPPs). CPPs are useful tools for efficiently transporting substances such as nucleic acids and proteins into cells.[11−14] Various CPPs have already been developed and are expected to be applied to the medical field.[15−18] We have succeeded in introducing proteins such as Citrine, bovine serum albumin, and green fluorescent protein into plant cells by complexing them with CPPs via ionic interactions.[11,19] This technique enabled us to impart transient kanamycin resistance to apple leaves by introducing a complex of CPP-fused peptide and neomycin phosphotransferase II (NPTII), a kanamycin resistance protein. Plant leaves receiving NPTII were selected after 2 days of incubation on a kanamycin-containing medium, whereas control leaves without NPTII started to die immediately after selection. However, the resistance was gradually lost after 2 days because the proteolytic degradation of bare NPTII occurred.[20] Therefore, a new carrier that can protect the cargo protein from proteases is required to impart transient traits to plants.

Polymeric vesicles have been studied as carriers to transport exogenic materials into living cells.[21,22] To date, many studies have reported materials acting as drug transport carriers to living bodies.[23,24] In addition, polymer vesicles have been developed as an enzymatic reaction chamber, similar to cells. Among the polymer vesicles, vesicles assembled from only hydrophilic copolymers have attracted much attention as enzymatic reactors because of their semipermeable membrane.[25−29] Kataoka et al. have developed polyion complex vesicles (PICsomes) as enzyme carriers constructed from a pair of oppositely charged block copolymers composed of PEG and polyamino acids.[30,31] PICsomes encapsulate proteins in their hollow interior and can be functionalized by functional molecules such as peptides. Macromolecules such as proteases hardly access the inside of the PICsome, which prevents the

Received: September 23, 2020
Revised: December 1, 2020
Published: December 14, 2020

https://dx.doi.org/10.1021/acs.biomac.0c01380
Biomacromolecules 2021, 22, 1080−1090

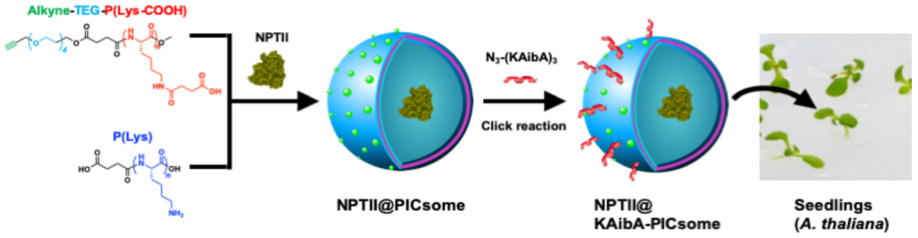

Figure 1. Schematic illustration of the development of PICsomes for the addition of functional traits to plants.

encapsulated proteins from proteolytic degradation. In contrast, small molecules such as enzyme substrates pass through the semipermeable membrane of the PICsomes. Therefore, enzymes encapsulated in PICsomes exhibit enzymatic activity in vivo with long-term durability.[32,33] A PICsome encapsulating β-galactosidase accumulated in the cancer cells, and the enzymatic reaction proceeded even after 4 days.[34] From these properties, PICsomes are expected to be carriers that maintain the activities of enzymes for a long period in vivo.

In this study, we developed a novel enzyme delivery system using a peptide-based PICsome to impart transient traits to plants for a longer period than the direct delivery of enzymes (Figure 1). We designed polyionic components based on tetra(ethylene glycol) (TEG) and peptides with alkyne groups on a terminus, namely, alkyne-TEG-P(Lys-COOH) and P(Lys), and the PICsome with alkyne groups on the surface was prepared by mixing in an aqueous solution. Modification with an appropriate CPP on the reactive alkyne groups enabled the PICsome to internalize into plant cells. With modification with CPPs, PICsomes containing NPTII were successfully introduced into plant cells, and the NTPII provided its function to the plants. This novel enzyme delivery system using PICsomes is a promising method for imparting long-term transient traits to plants without genetic modification, which enables application of the modified plants in various environments.

EXPERIMENTAL SECTION

Materials. Chemical reagents were obtained from Tokyo Chemical Industry Co., Ltd. (Tokyo, Japan), Watanabe Chemical Industries Ltd. (Hiroshima, Japan), Fujifilm Wako Pure Chemical Industries, Ltd. (Osaka, Japan), and Sigma-Aldrich (St. Louis, MO) and used without further purification. Papain (EC No. 3.4.22.2) was purchased from Fujifilm Wako Pure Chemical Industries, Ltd. (Osaka, Japan) and used as received. Trypsin was purchased from Sigma-Aldrich (St. Louis, USA). Peptides with an azide-modified *N*-terminus, N_3-BP100 (N_3-KKLFKKILKYL-OH) and N_3-KAibA (N_3-KXAKXAKXA-OH; X = Aib), were obtained from Eurofins Genomics K.K. (Tokyo, Japan).

Characterization Procedures. Dynamic light scattering (DLS) measurements were performed using a Zetasizer Nano ZS (Malvern Instruments Ltd., Malvern, UK) instrument with an incident He−Ne laser (633 nm). Matrix-assisted laser desorption/ionization time-of-flight (MALDI-TOF) mass spectra were obtained using an Autoflex speed spectrometer (Bruker Daltonics, Billerica, MA) in a linear/positive mode with α-cyano-4-hydroxycinnamic acid (α-CHCA) as a matrix. ^{1}H nuclear magnetic resonance (NMR) spectra (500 MHz) were recorded using a Varian NMR spectrometer (Varian Medical Systems, Palo Alto, CA). Deuterium oxide (D_2O) was used as the solvent.

Synthesis of Poly(Lys-Boc). To polymerize N_ε-Boc-protected L-lysine methyl ester, we used chemoenzymatic polymerization according to the previous literature.[35,36] A solution of N_ε-Boc-protected L-lysine methyl ester hydrochloride (5 g, 16.8 mmol) in phosphate buffer (8.4 mL, 1.0 M, pH = 8.0) was placed in a glass tube equipped with a stirring bar. To this was added a solution of papain (0.84 g) in phosphate buffer (5.6 mL) in one portion. The final concentrations of lysine and papain were 1.0 M and 50 mg mL^{-1}, respectively, in a total volume of 16.8 mL. The mixture was stirred at 800 rpm and 40 °C for 4 h using an EYELA ChemiStation PPS-5511 (Tokyo Rikakikai Co. Ltd., Tokyo, Japan). After cooling to room temperature, the precipitate was collected by centrifugation at 9000 g and 4 °C for 15 min. The crude product was washed twice with deionized water, centrifuged, and lyophilized to give poly(Lys-Boc) with a methyl ester terminus as a white powder. The yield was 0.62 g (12.4%). MALDI-TOF-MS (matrix: α-CHCA): *m/z*: 1196 [5 mer + Na]$^+$, 1424 [6 mer + Na]$^+$, 1653 [7 mer + Na]$^+$.

Synthesis of Alkyne-TEG-OH. A solution of TEG (7.04 g, 36.2 mmol) and potassium *tert*-butoxide (4.11 g, 36.6 mmol) in tetrahydrofuran (THF, 70 mL) was added to a flask equipped with an addition funnel and a stirring bar. A solution of propargyl bromide (3.0 mL, 39.6 mmol) in THF (10 mL) was added dropwise, and the mixture was stirred at room temperature for 24 h. After the reaction, the inorganic salt was filtered off, and THF was removed using a rotary evaporator. Chloroform was added to the crude product, and the solution was washed with water and saturated NaCl solution. The organic layer was dried with $MgSO_4$ and concentrated using a rotary evaporator. The title compound was obtained by drying under vacuum as a yellow liquid. The yield was 3.77 g (44.8%). ^{1}H-NMR (500 MHz, $CDCl_3$): δ 2.42 (t, 1H), 3.60 (m, 2H), 3.64−3.75 (m, 14H), 4.20 (d, 2H).

Synthesis of Alkyne-TEG-COOH. Succinic anhydride (2.03 g, 20.3 mmol) was added to a solution of alkyne-TEG-OH (3.77 g, 16.2 mmol), diisopropylethylamine (2.11 g, 16.3 mmol), and 4-(*N*,*N*-dimethylamino)pyridine (0.11 g, 0.9 mmol) in dichloromethane (14.1 mL) in a flask equipped with a stirring bar, and the mixture was stirred at room temperature for 24 h. The mixture was washed with 10% $KHSO_4$ aq. solution and saturated NaCl solution. The organic layer was dried with $MgSO_4$ and concentrated using a rotary evaporator. The resulting liquid was dried under vacuum to afford the title compound and used for the next reaction without further purification. The crude yield was 3.43 g (63.8%). ^{1}H-NMR (500 MHz, $CDCl_3$): δ 2.42 (t, 1H), 2.66 (m, 4H), 3.64−3.75 (m, 14H), 4.20 (d, 2H).

Synthesis of Alkyne-TEG-Poly(Lys-Boc). A solution of poly(Lys-Boc) (0.480 g, 0.337 mmol), alkyne-TEG-COOH (1.16 g, 3.49 mmol), and triethylamine (0.354 g, 3.50 mmol) in dichloromethane (15 mL) was placed in a flask equipped with a stirring bar. To this, 1-ethyl-3-(3-dimethylaminopropyl)carbodiimide (EDC) hydrochloride (0.670 g, 4.31 mmol) was added, and the mixture was stirred at room temperature for 24 h. After the reaction, dichloromethane was removed using a rotary evaporator, and the crude product was dissolved in a small amount of methanol. The solution was poured in deionized water, and the precipitate was filtered and washed with water. The title compound was obtained after drying under vacuum as a white powder. The yield was 0.236 g (44.6%). MALDI-TOF-MS (matrix: α-CHCA): *m/z*: 1524 [5 mer + K]$^+$, 1751 [6 mer + K]$^+$, 1981 [7 mer + K]$^+$.

Synthesis of Alkyne-TEG-polyLys. A solution of alkyne-TEG-poly(Lys-Boc) (0.234 g, 0.136 mmol) in dichloromethane (5 mL) was placed in a flask equipped with a stirring bar. Trifluoroacetic acid (5 mL) was added to this solution, and the resulting mixture was stirred at room temperature for 2 h. After the reaction, all the solvent

https://dx.doi.org/10.1021/acs.biomac.0c01380
Biomacromolecules 2021, 22, 1080−1090

was removed by vacuum distillation, and diethyl ether (20 mL) was added to the crude product. The precipitate was collected by decantation of the supernatant solution and then was washed with diethyl ether two times. The solid was dried under vacuum. A white solid was obtained after lyophilizing the dialyzed solution. MALDI-TOF-MS (matrix: α-CHCA): *m/z*: 1008 [5 mer + Na]$^+$, 1137 [6 mer + Na]$^+$, 1265 [7 mer + Na]$^+$.

Synthesis of Alkyne-TEG-Poly(Lys-COOH). A solution of alkyne-TEG-polyLys (10 mg, 8.98 μmol) and triethylamine (0.1 g) in *N*,*N*-dimethylformamide (DMF) (0.5 mL) was added to a flask equipped with a stirring bar. A solution of succinic anhydride (0.108 g, 1.08 mmol) in DMF (0.5 mL) was added, and the mixture was stirred at room temperature for 6 h. After the reaction, ethyl acetate was added, and the precipitate was collected by centrifugation at 9000 g and 4 °C for 15 min. The precipitate was washed with ethyl acetate twice. After drying, the crude product was dissolved in 100 mM acetate buffer (pH 5.0) and lyophilized. The obtained white solid was washed with 99.5% ethanol three times and dried under vacuum. MALDI-TOF-MS (matrix: α-CHCA): *m/z*: 1524 [5 mer + K]$^+$, 1751 [6 mer + K]$^+$, 1981 [7 mer + K]$^+$.

Synthesis of P(Lys). Alkyne-TEG-polyLys (10 mg, 8.98 μmol) was dissolved in a 10 mM triethylamine aqueous solution, and the solution was heated at 40 °C for 1 h. After the reaction, the solution was dialyzed against water (MWCO: 100 kDa) for 24 h and lyophilized to afford a white powder. MALDI-TOF-MS (matrix: α-CHCA): *m/z*: 759 [5 mer + H]$^+$, 888 [6 mer + H]$^+$, 1017 [7 mer + H]$^+$.

Preparation of PICsomes. Alkyne-TEG-P(Lys-COOH) and P(Lys) were dissolved in Milli-Q. These solutions were filtered using a 0.22 μm membrane filter before mixing. These solutions (100−1000 μM) were mixed in the ratio of NH_2 to COOH fixed at 1:1, and the mixture was vortexed for 10 s and incubated at 25 °C for 10 min.

Preparation of Cross-Linked PICsomes and Calculation of the Cross-Linking Efficiency. A PICsome solution (200 μM, 6 mL) was mixed with EDC solutions of various concentrations to obtain cross-linked PICsomes at [EDC]/[NH_2] ratios of 1, 2, 3, 5, 10, and 20. The solution was incubated at 25 °C for 3 h. After the reaction, EDC was removed by dialysis (MWCO: 100 kDa) for 2 h. The dialyzed solution was lyophilized. The lyophilized powder was dissolved in 600 μL of D_2O. The cross-linking rate was calculated from the ^{1}H-NMR spectra of the mixture, which were recorded (Varian Medical Systems, Palo Alto, CA) at 25 °C at a frequency of 500 MHz.

Field-Emission Scanning Electron Microscopy (FESEM) Observation. A PICsome solution (200 μM, 5 μL) or a cross-linked PICsome solution at [EDC]/[NH_2] ratios of 1, 2, 3, 5, 10, and 20 (5 μL) was dropped on a silicon wafer, incubated for 1 min, and dried in vacuo. The wafer was analyzed by FESEM (GeminiSEM 300, Carl Zeiss) with an acceleration voltage of 1 kV. For cross-sectional scanning electron microscopy (SEM) imaging, the PICsomes (200 μM, 100 μL) were cross-linked with EDC at [EDC]/[NH_2] = 1 for 3 h. After the cross-linking reaction, the solution was mixed (1:1) with a low-melting agarose. The mixture was allowed to solidify at 25 °C for 30 min and dehydrated by immersion in methanol and propylene oxide. The agarose was embedded in an epoxy resin (Epon 812, TAAB Laboratories Equipment Ltd., Berkshire, UK) and cut with a microtome (PowerTome, RMC products, India) into slices with a thickness of 100 nm. Each section was stained with 4% samarium chloride for 30 min and lead citrate for 5 min and dried at 25 °C. Before observation, each section was coated with carbon.

Preparation of Rhodamine-Labeled NPTII (RhB-NPTII). An NPTII solution (10 mg mL^{-1}) in 100 mM sodium carbonate solution (pH 9.0) was prepared, and 100 μL of this solution was mixed with 10 μL of RhB (10.0 g L^{-1}) in dimethyl sulfoxide and reacted at 25 °C for 12 h. After the reaction, the mixture was purified by gel filtration chromatography using a Sephadex G-25 column (Sigma-Aldrich) at 25 °C.

Encapsulation of NPTII into PICsomes. An aqueous solution of alkyne-TEG-P(Lys-COOH) (50 μL, 200 μM) was mixed with 1 μL of a 1 or 10 mg mL^{-1} solution of NPTII with or without RhB labeling in 100 mM Bis−Tris buffer (pH 7.0). An aqueous solution of P(Lys) (50 μL, 200 μM) was added to this solution. The mixture was vortexed for 10 s and incubated at 25 °C for 10 min. Then, 1 μL of EDC aqueous solution was added to this mixture and reacted for 3 h to cross-link PICsomes at [EDC]/[NH_2] = 1. The remaining EDC and free protein were removed by dialysis (MWCO: 100 kDa) against 1 mM Bis−Tris buffer (pH 7.0) for 6 h at 25 °C.

Fluorescence Correlation Spectroscopy (FCS) Analysis for PICsomes Containing NPTII. FCS measurements were carried out using a confocal laser microscope LSM880 (Carl Zeiss) using a 488 nm laser. The sample solution (15 μL) was dropped on a cover glass (Carl Zeiss) and analyzed at 25 °C. Fitting was performed using ZEN 2.3 SP1 operating software (Carl Zeiss). The autocorrelation function *G*(t) was obtained using the following equation[37]

$$G(t) = 1 + \frac{1}{N} \times \frac{1}{\left(1 + \frac{t}{\tau}\right)\sqrt{1 + \frac{1}{k^2}\cdot\frac{t}{\tau}}} \times \left(\frac{1 + F\exp\left(\frac{t}{\tau_{trip}}\right)}{1 - F}\right) \quad (1)$$

where *N* is the number of molecules, *t* is the correlation time, τ is the diffusion time of the component, *k* is a structural constant, *F* is the fraction of particles that have entered the triplet state, and τ_{trip} is the relaxation time of the corresponding triplet state.

Evaluation of the Activity of NPTII. The enzyme activity in vitro was measured using the Fluorospark Kinase/ADP Multi-Assay Kit (Fujifilm Wako Pure Chemical Corporation, Japan). The detection reagent was prepared by mixing solutions of substrate, resazurin, enzyme, and reductant blocker at 90:1:5:4. Kanamycin (10 mg L^{-1}) and adenosine triphosphate (ATP) were added to the detection reagent. For the determination of enzymatic activity, the ATP concentration was varied between 1 and 200 μM. Reactions were initiated by adding 25 μL of a solution of NPTII encapsulated in PICsomes (NPTII@PICsomes) to 25 μL of the detection reagent containing kanamycin and ATP. The fluorescence signal from resorufin at each time point was measured at Ex 540 nm/Em 590 nm using a SpectraMax instrument (Molecular Devices, CA) for 9 h. The kinetic constants K_m and V_{max} were calculated using the Michaelis−Menten equation.

Evaluation of the Proteolytic Resistance of NPTII. Trypsin solution (8 μg mL^{-1}) was added to the NPTII@PICsome solution and incubated at 25 °C. For the determination of proteolytic resistance, the reaction time was varied from 10 min to 2 h. After the reaction, the enzyme activity in vitro was measured using the Fluorospark Kinase/ADP Multi-Assay Kit. The detection reagent was prepared by mixing solutions of substrate, resazurin, enzyme, and reductant blocker at 90:1:5:4. The resulting reaction mixture was added to the detection reagent for measurement of the enzyme activity. The fluorescence signal from resorufin was measured at Ex 540 nm/Em 590 nm.

Functionalization with BP100 on PICsomes. An aqueous solution of alkyne-TEG-P(Lys-COOH) (50 μL, 200 μM) was mixed with P(Lys) (50 μL, 200 μM). The mixture was vortexed for 10 s and incubated at 25 °C for 10 min. After incubation, an aqueous solution (1 μL) of the click reagents $CuSO_4$ (1 mM), tris-(benzyltriazolylmethyl)amine (THPTA, 6 mM), sodium ascorbate (50 mM), and 0.5 μL of N_3-BP100 solution (5 mM) was added to 100 μL of the PICsome solution, and the mixture was reacted at 25 °C for 30 min. DLS measurement of this mixture solution was performed without dialysis.

Functionalization with KAibA on Cross-Linked PICsomes Containing NPTII. An aqueous solution of alkyne-TEG-P(Lys-COOH) (50 μL, 200 μM) was mixed with 1 μL of a 1 or 10 mg mL^{-1} solution of RhB-NPTII or NPTII in 100 mM Bis−Tris buffer (pH 7.0). An aqueous solution of P(Lys) (50 μL, 200 μM) was added to this solution. The mixture was vortexed for 10 s and incubated at 25 °C for 10 min. After incubation, 1 μL of EDC aqueous solution was added to this mixture and reacted for 3 h to cross-link PICsomes at

https://dx.doi.org/10.1021/acs.biomac.0c01380
Biomacromolecules 2021, 22, 1080−1090

[EDC]/[NH_2] = 1. The remaining EDC and free protein were removed by dialysis using a cellulose ester tube (MWCO: 100 kDa) against 1 mM Bis−Tris buffer (pH 7.0) at 25 °C for 3 h. An aqueous solution (1 μL) of the click reagents $CuSO_4$ (1 mM), THPTA (6 mM), sodium ascorbate (50 mM), and 0.5 μL of N_3-KAibA solution (5 mM) was added to 100 μL of the PICsome solution, and the mixture was reacted at 25 °C for 30 min. After the reaction, the solution was dialyzed against 1 mM Bis−Tris buffer (pH 7.0) at 25 °C for 3 h. The reaction efficiency was determined by reversed-phase high-performance liquid chromatography (RP-HPLC) without NPTII. RP-HPLC analyses were performed using an HPLC system consisting of an AS-2055 autosampler, a PU2089 gradient pump, a CO-4060 column oven, and a UV-4075 UV/vis detector (JASCO) using a YMC-Triart C18 column (particle size 5 μm, 150 × 3 mm, YMC, Kyoto, Japan) with a flow rate of 1 mL min^{-1} at 25 °C. *tert*-Butoxycarbonyl(Boc)-Gly was used as an internal standard. For analyses of the CPP modification efficiency, 50 μL of the click reaction mixture with Boc-Gly was injected and eluted using a mixed mobile phase with a linear gradient of CH_3CN/water containing 0.1% TFA (5/95 to 52.5/47.5 over 47.5 min).

Plant Growth Conditions. Seedlings of *Arabidopsis thaliana* (*A. thaliana*) (accession Col-0) were used for all experiments involving PICsome internalization into plants. The seeds of *A. thaliana* were sown on 1% agar medium containing a 0.5 Murashige and Skoog (MS) medium without sucrose and then incubated in a plant incubator (Biotron NK System, Nippon Medical & Chemical Instruments Co. Ltd., Osaka, Japan) under 16 h day/8 h night cycles, 100 μmol m^{-2} s^{-1}, and 22 °C for 2 days.

Internalization of KAibA-Modified PICsomes Containing NPTII into *A. thaliana*. RhB-NPTII-containing KAibA-modified PICsomes (RhB-NPTII@KAibA-PICsomes), RhB-NPTII-containing PICsomes (RhB-NPTII@PICsomes), and RhB-NPTII (0.1 mg/mL) were prepared and dialyzed against 1 mM Bis−Tris buffer (pH 7.0) at 25 °C for 6 h. For the internalization of NPTII into *A. thaliana*, 14 seedlings were immersed in 140 μL of dialyzed solution of RhB-NPTII@KAibA-PICsome, RhB-NPTII@PICsome, or RhB-NPTII in a 2 mL microtube, degassed at −0.08 MPa for 1 min, and then pressurized at 0.08 MPa for 1 min. After internalization, the solution was removed, and these seedlings were incubated on 0.5 MS culture plates without sucrose for 24 h. The internalization of RhB-NPTII@KAibA-PICsomes was confirmed by confocal laser scanning microscopy (CLSM, Zeiss LSM880). Observation of PICsome internalization in plants was performed by CLSM using an LSM880 instrument (Carl Zeiss, Oberkochen, Germany). Images were acquired at excitation wavelengths of 405 nm (for calcofluor white) and 561 nm (for rhodamine B, RhB) and visualized under a 63× oil immersion objective. The colocalization analysis of micrographs was performed using the Zen 2.3 SP1 operating software (Carl Zeiss). The cell walls of these seedlings were stained with a 0.1 g L^{-1} aqueous solution of calcofluor white for 30 min before the CLSM observation. To evaluate the stability of NPTII inside the plant cells, CLSM observation of seedlings was performed at 1, 2, 3, 4, 5, 6, 7, 10, 14, and 18 days.

Kanamycin Selection. Fourteen *A. thaliana* seedlings were immersed in a 140 μL solution of NPTII@KAibA-PICsomes, NPTII, or 1 mM Bis−Tris buffer in a 2 mL microtube, degassed at −0.08 MPa for 1 min, and pressurized at 0.08 MPa for 1 min. The seedlings were placed and grown on the MS medium containing 10 mg L^{-1} of kanamycin and a 0.01% plant preservative mixture, a set of biocides/fungicides for plant culture (Plant Cell Technology, USA). We used a plastic sheet to prevent leaves from sticking to the medium. After 1 week, the seedlings were freeze-dried, and the dry weights of the seedlings were measured. The experiment was replicated five times, and the significance of the differences among the dry weights of plants was determined using the Mann−Whitney test. The differences were considered statistically significant at $P < 0.05$.

RESULTS AND DISCUSSION

We developed a new enzyme delivery system using a peptide-based PICsome that can maintain long-term enzymatic activity in plants. We synthesized peptide-based polyions for the formation of PICsomes to deliver enzymes into plants (Figure 1). As a precursor of the polycation component, poly(Lys-Boc) was prepared by papain-catalyzed chemoenzymatic polymerization,[38,39] and the average degree of polymerization was found to be 6 by characterization using MALDI-TOF-MS and ^{1}H NMR spectroscopy.[40,41] Kataoka et al. reported that the polyion complex favors vesicle (PICsome) formation when the volume fraction of hydrophilic PEG is lower than 10%, whereas increasing the PEG fraction to more than 10% makes the polyion complex form micelles.[42] Therefore, TEG was adopted in this study to obtain the appropriate composition between poly(Lys) and TEG in block structures. Alkyne-TEG-PLys was obtained by condensation of alkyne-TEG-COOH and P(Lys-Boc) followed by deprotection of the Boc groups on the side chain. As an anionic component, alkyne-TEG-P(Lys-(COOH)) was synthesized by a reaction of alkyne-TEG-PLys and succinic anhydride. PLys was obtained by hydrolysis of alkyne-TEG-PLys using triethylamine.

The self-assembling behavior of the complex obtained from these peptides was investigated by DLS and FESEM. Solutions of the peptides were mixed at a molar ratio of 1:1 and incubated for 10 min, and the z-average diameter of the particles was estimated by DLS. At concentrations less than 100 μM, no specific assembly was formed. At concentrations above 100 μM, nanoassemblies were obtained, and the sizes of these assemblies were in the range of 100−950 nm according to DLS (Table 1). The z-average diameter of the assemblies

Table 1. Dependences of the Diameter and Polydispersity Index (PDI) of the Assembly on Peptide Concentration as Obtained by DLS

[peptide]/μM	z-average diameter/nm[a]	PDI[a]
1000	952 ± 11	0.225 ± 0.041
500	350 ± 16	0.234 ± 0.009
200	141 ± 3	0.122 ± 0.004
100	216 ± 1	0.230 ± 0.002

[a]Values were determined by DLS measurements and are shown as mean ± standard deviation (n = 3).

increased with the increasing peptide concentration. At peptide concentrations greater than 500 μM, the diameter increased over time, and the solutions became turbid. In contrast, the peptide assemblies with sizes of 150−200 nm formed at 100 and 200 μM peptide concentrations stably maintained their sizes up to 12 h. An FESEM image of the peptide shows a spherical assembly at 200 μM (Figure 2), where the size of the particles corresponds to the z-average diameter estimated by DLS. These results indicate that a stable spherical assembly was formed by mixing solutions of cationic and anionic peptides at 100−200 μM. Smaller assemblies are more suitable for transportation in plants because they more easily penetrate the cell wall.[43] Therefore, spherical assemblies prepared at 200 μM were used for subsequent experiments.

Kishimura et al. reported that polyionic block copolymer components forming PICsomes can be stabilized by a cross-linking reaction using condensing agents such as glutaraldehyde and EDC.[31,44] Accordingly, in this study, the peptides that compose the PICsomes were cross-linked using EDC after

https://dx.doi.org/10.1021/acs.biomac.0c01380
Biomacromolecules 2021, 22, 1080−1090

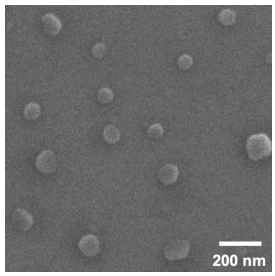

Figure 2. FESEM image of an assembly obtained from the mixed solution of peptides at 200 μM.

PICsome formation. The cross-linking efficiency was calculated from the peak shift of the methylene protons adjacent to the primary amino group in the side chain of poly(Lys) from 2.8 to 3.1 ppm in the ^{1}H NMR spectrum (Figure 3). The cross-linking efficiencies at various concentrations of EDC for the primary amine in the cationic peptide are shown in Table 2. The cross-linking efficiency increased with increasing EDC and saturated at [EDC]/[NH_2] = 10. The z-average diameters of the cross-linked PICsomes were estimated by DLS, as shown in Table 2. The diameter and PDI obtained from DLS increased as the concentration of EDC increased. FESEM images of cross-linked PICsomes show that monodisperse spherical assemblies were obtained at [EDC]/[NH_2] = 1 and 2 (Figure 4). However, aggregation of PICsomes was observed at large excesses of the condensing agent, for example, [EDC]/

Table 2. Z-Average Diameter, PDI, and Cross-Linking Efficiency of the Cross-Linked PICsomes Obtained by DLS[a]

[EDC]/[NH_2]	z-average diameter/nm[b]	PDI[b]	cross-linking efficiency/%[c]
1	181 ± 4	0.128 ± 0.008	28
2	211 ± 7	0.186 ± 0.008	45
3	229 ± 4	0.239 ± 0.006	56
5	272 ± 4	0.284 ± 0.024	72
10	352 ± 41	0.358 ± 0.019	93
20	382 ± 34	0.385 ± 0.015	89

[a]The assemblies were cross-linked with EDC at a [EDC]/[NH2] ratio ranging from 1 to 20. [b]Values were determined by DLS measurements and are shown as mean ± standard deviation (n = 3). [c]Values were calculated from the decrease in the peak of methylene protons adjacent to the primary amino group in the side chain of poly(Lys) in the NMR spectrum.

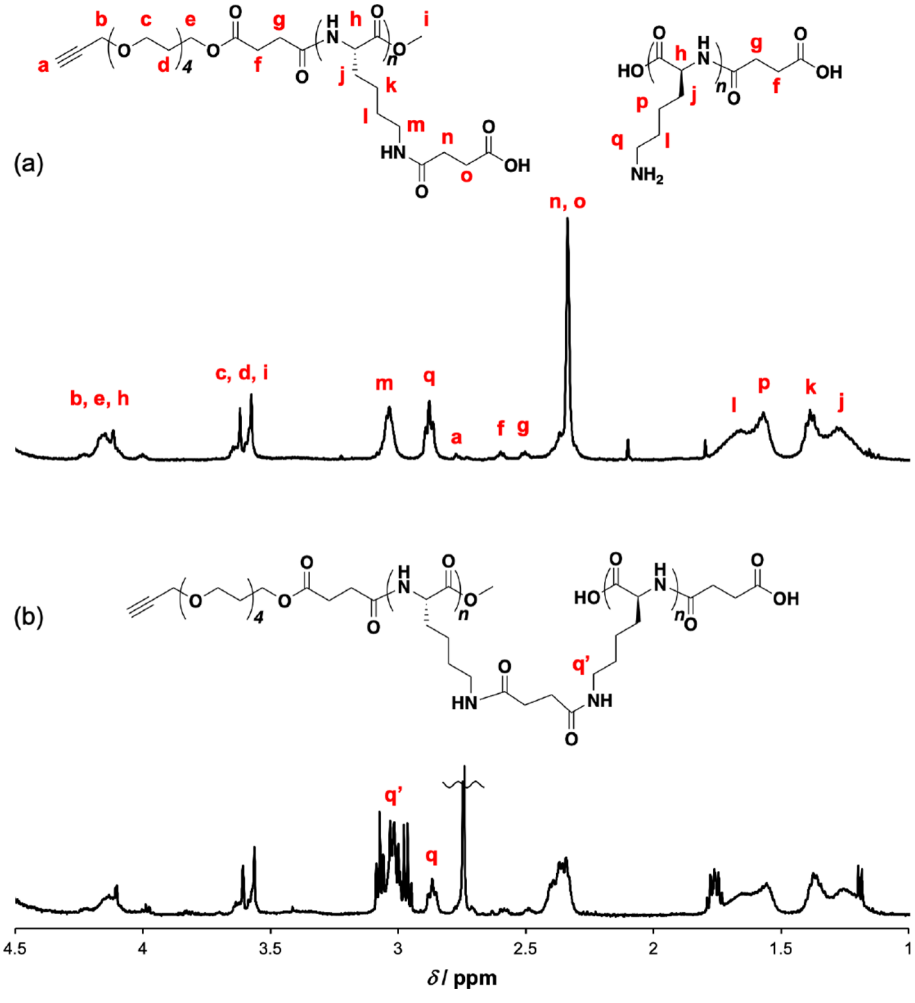

Figure 3. ^{1}H NMR spectra of a mixture of alkyne-TEG-P(Lys-COOH) and P(Lys) before (a) and after (b) the cross-linking reaction with EDC at [EDC]/[NH_2] = 1. After cross-linking of the side chain of alkyne-TEG-P(Lys-COOH) and P(Lys), the peak at q shifted to q′.

https://dx.doi.org/10.1021/acs.biomac.0c01380
Biomacromolecules 2021, 22, 1080−1090

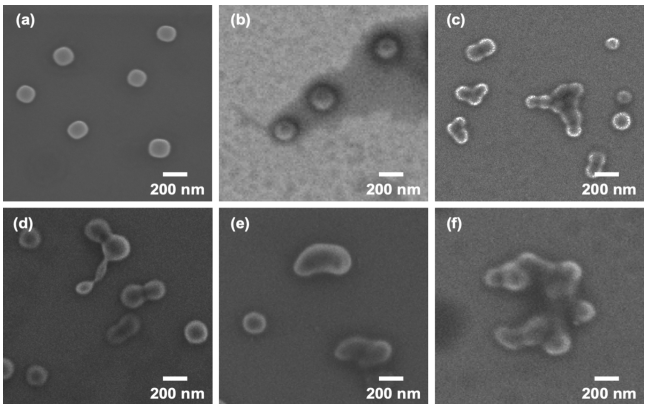

Figure 4. FESEM images of spherical assemblies prepared from alkyne-TEG-P(Lys-COOH) and P(Lys) after cross-linking with EDC at [EDC]/[NH_2] = 1 (a), 2 (b), 3 (c), 5 (d), 10 (e), and 20 (f).

[NH_2] = 3. This result is consistent with the DLS results, indicating that the PICsomes were aggregated by a cross-linking reaction between the PICsome surface above [EDC]/[NH_2] = 3. The assembly cross-linked at [EDC]/[NH_2] = 1 was embedded in an epoxy resin and then ultrathin-sectioned for FESEM observation of the cross-section of the assembly. The cross-sectional SEM image of the assembly shows many spherical morphologies with hollow structures (Figure 5). The

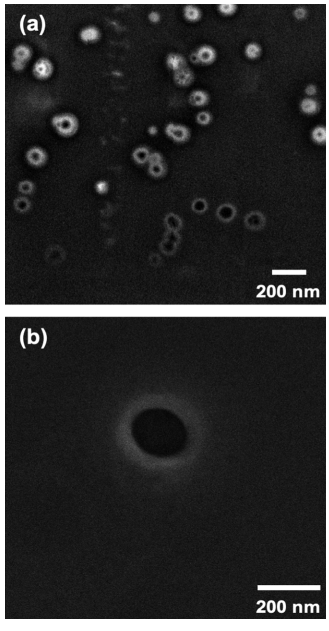

Figure 5. Cross-sectional SEM images of hollow structures prepared by mixing alkyne-TEG-P(Lys-COOH) and P(Lys) under low (a) and high (b) magnifications. The PICsomes were cross-linked at [EDC]/[NH_2] = 1.

diameter of the PICsome observed in the SEM image is consistent with those obtained from DLS. Therefore, these results indicate that mixing the polyionic peptides provided a stable vesicle-type assembly, namely, a PICsome, after the cross-linking reaction.

Next, we investigated the availability of the PICsomes as a delivery platform that encapsulates an enzyme to maintain its activity in plants. NPTII was used as a model enzyme that functions in plants. NPTII detoxifies kanamycin, which is toxic to plants, by transferring the phosphate group of ATP to kanamycin. The encapsulation of NPTII in the PICsomes was evaluated by FCS. FCS measures the diffusion time of a fluorescent molecule. The apparent diffusion time of a fluorescent molecule increases when the fluorescent molecule is encapsulated in the hollow interior of the PICsome.[31] For FCS measurements, NPTII was labeled with RhB isothiocyanate according to a previous report.[20] The RhB-modified NPTII (RhB-NPTII) was then encapsulated into PICsomes by mixing peptides in the presence of RhB-NPTII. After the PICsomes were cross-linked using EDC, free RhB-NPTII and EDC were removed by dialysis. An autocorrelation obtained for RhB-NPTII before and after encapsulation by PICsomes is shown in Figure 6. The blue curve is the autocorrelation function of NPTII only (Figure 6a), whereas the red curve represents the PICsomes formed in the presence of NPTII (Figure 6b). The autocorrelation curve of RhB-NPTII in the presence of PICsomes can be fitted by a single-component equation. Therefore, free RhB-NPTII did not exist in the solution after dialysis. Normalized FCS curves show that the diffusion time of RhB-NPTII in the presence of PICsome was larger than that of RhB-NPTII only (Figure 6c). The apparent hydrodynamic diameter was calculated using the Stokes–Einstein equation, and the diffusion time of RhB-NPTII was obtained by FCS curve fitting. Mixing RhB-NPTII with the PICsome-forming peptides changed the apparent hydrodynamic diameter from 9.4 to 230 nm, which is close to the value for these PICsomes estimated by DLS. These results indicated that all RhB-NPTII were encapsulated into PICsomes, leaving no free RhB-NPTII.

The enzymatic activity of NPTII@PICsomes was evaluated by assessing the phosphorylation of kanamycin in vitro. Various concentrations of ATP and 10 mg L^{-1} kanamycin were added to the NPTII@PICsomes in aqueous solutions, and the time-dependent changes in the fluorescence intensity of the resulting resorufin product were obtained as relative fluorescence units (RFUs). The initial rate of this reaction was calculated from the rate of the increase in RFUs for the first 15 min. The obtained initial reaction rate was plotted against the ATP concentration (Figure 7). The Michaelis constant K_m and the maximum rate V_{max} were determined from these curves using the Michaelis–Menten equation (Table 3). NPTII exhibited enzymatic activity in the presence of PICsomes. The K_m of NPTII increased 1.5-fold in the presence of PICsomes. In the Michaelis–Menten kinetics, K_m is an index for the binding constant between an enzyme and a substrate when the binding rate is sufficiently faster than the enzyme reaction rate. Therefore, K_m can be interpreted as the substrate affinity and an increase in K_m means a decrease in the affinity of the enzyme for its substrate. The change of K_m in the current system indicates that the activity of NPTII decreased by the encapsulation in PICsomes. Such a degree of change in K_m has also been reported by Kataoka et al.[36] In that work, the K_m value of β-galactosidase loaded in PICsomes was twice that of free β-galactosidase. They attributed the decrease in K_m to a difference in the accessibility of the enzyme to substrates or to a slight inhibition of product release by the barrier of the PICsome membrane.

To evaluate the proteolytic resistance of NPTII, the activities of NPTII alone and NPTII@PICsomes in the presence of kanamycin were measured using a kinase assay after treatment with trypsin as a model protease. After NPTII and NPTII@PICsomes were incubated with trypsin (8 μg

https://dx.doi.org/10.1021/acs.biomac.0c01380
Biomacromolecules 2021, 22, 1080–1090

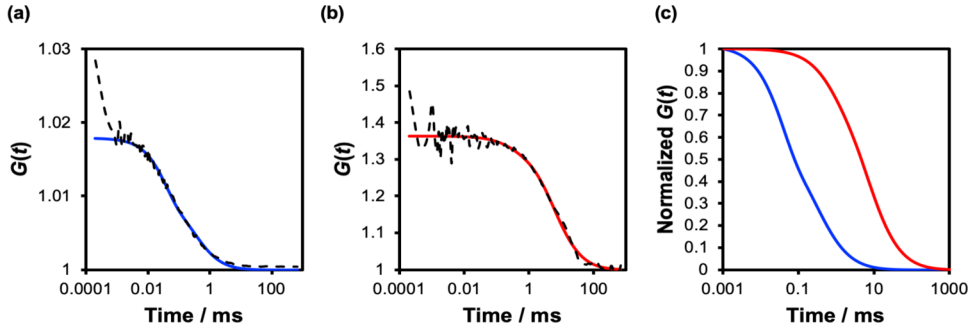

Figure 6. Measured (dot) and fitted (solid) autocorrelation curves of RhB-NPTII (a) and RhB-NPTII in the presence of PICsomes (b) measured by FCS. The fitting curve was obtained using a single-component equation (eq 1). (c) Normalized autocorrelation curves of RhB-NPTII (blue) and RhB-NPTII in the presence of PICsomes (red). These curves were normalized at 1 μs to compare the diffusion times obtained from these curves.

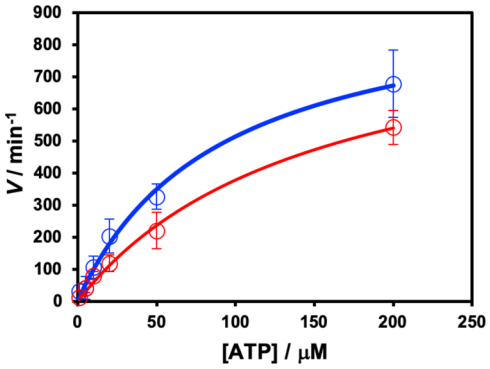

Figure 7. Michaelis−Menten plots of the NPTII activity in the presence (red) or absence (blue) of PICsomes. NPTII was reacted with 10 mg L^{-1} of kanamycin at ATP concentrations ranging from 1 to 200 μM. The error bars show the standard deviation determined by three measurements.

Table 3. K_m and V_{max} Values of NPTII in the Absence or Presence of PICsomes Obtained using the Michaelis−Menten Equation

	K_m (ATP)/μM	V_{max}/min^{-1}
NPTII only	90	977
NPTII@PICsome	149	945

mL^{-1}) at 25 °C for 0−2 h, the enzymatic activity was measured as a function of reaction time (Figure 8). The fluorescence intensity of NPTII dramatically decreased after treatment with trypsin, indicating that the apparent activity decreased due to the proteolytic degradation of NPTII. In contrast, NPTII@PICsomes showed a slight decrease in the fluorescence but still maintained the enzymatic activity after 2 h of incubation with trypsin. Additionally, the decrease rate of the activity of NPTII@PICsome was smaller than that of NPTII alone. These results indicate that encapsulation in PICsomes can protect NPTII from proteolytic degradation and maintain the enzymatic function of NPTII. The FCS measurements of RhB-NPTII@PICsomes showed that non-encapsulated NPTII did not exist in those solutions. These results support NPTII being encapsulated into PICsomes. In addition, the enzyme activity measurements revealed that the encapsulated NPTII maintained its enzymatic activity.

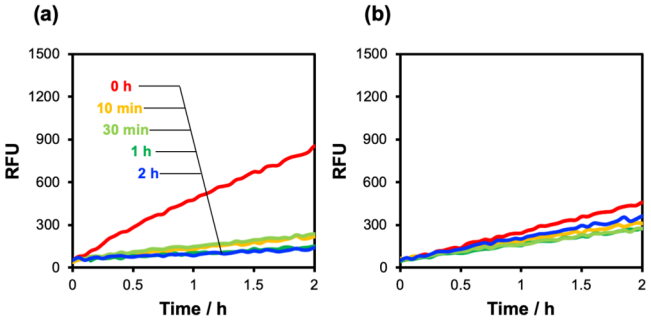

Figure 8. NPTII activity in the absence (a) or presence (b) of PICsomes after treatment with 8 μg mL^{-1} of trypsin.

The introduction of PICsomes containing NPTII, which exhibited enzymatic activity and proteolytic resistance, into plants is expected to impart kanamycin resistance to plants without gene modification. To deliver PICsomes containing NPTII into plant cells, the PICsomes need to penetrate the cell membrane. Therefore, CPPs were added on the periphery of the PICsomes via a click reaction using an alkyne group at the terminus of the TEG block. We attempted to modify the PICsomes with two types of CPPs, BP100 and KAibA peptides. BP100 (KKLFKKILKYL) is a CPP that has been used for gene delivery into plants by complexation with plasmid DNA,[45] whereas KAibA (KXAKXAKXA, X = Aib) was developed as a CPP applicable to both animal and plant cells with a long-term cell-penetrating ability.[46] After the PICsomes containing NPTII were prepared, the azide-modified CPPs, N_3-BP100 or N_3-KAibA, were introduced via a click reaction. The PICsomes were reacted with N_3-BP100 (25 μM, 0.25 equiv against the alkyne of the peptide before dialysis), which resulted in BP100-modified PICsomes that were shown by DLS to form large aggregates (Table 4). This is because BP100 has a large number of positive charges at natural pH, leading to

Table 4. Dependences of the z-Average Diameter and PDI of the CPP-PICsomes Containing NPTII on the N_3-BP100 or N_3-KAibA Concentration, as Obtained from DLS

CPP	[peptide]/μM	z-average diameter/nm[a]	PDI[a]
N_3-BP100	25	1203 ± 70	0.340 ± 0.056
N_3-KAibA	50	390 ± 7	0.400 ± 0.043
	25	143 ± 2	0.192 ± 0.011
	12.5	164 ± 2	0.215 ± 0.008
	5	157 ± 1	0.195 ± 0.010

[a]Values were determined by DLS measurements and are shown as mean ± standard deviation (n = 3).

https://dx.doi.org/10.1021/acs.biomac.0c01380
Biomacromolecules 2021, 22, 1080−1090

the collapse of the PICsomes by interactions with the polyanionic peptide in the assembly. Thus, we used the N_3-KAibA peptide. The KAibA peptide is an amphiphilic peptide that adopts a stable helical structure and has only three positive charges in its nine residues. Modification with the KAibA peptide does not inhibit the formation of the PICsomes. Thus, after NPTII was encapsulated, the PICsomes were modified with N_3-KAibA via a click reaction. The dependence of the resulting assembly morphology on the N_3-KAibA concentration was evaluated by DLS and SEM (Table 4). At an N_3-KAibA concentration of 50 μM, the diameter of the assembly was approximately 400 nm, indicating that the large amount of N_3-KAibA negatively affects the formation of the PICsomes, similar to the case of BP100. At less than 25 μM N_3-KAibA, the assembly maintained a diameter corresponding to that before the reaction. In addition, the FESEM images indicated a spherical morphology (Figure S1). From these results, it was clarified that the size and morphology were maintained at KAibA concentrations below 25 μM. Therefore, in subsequent experiments, a KAibA concentration of 25 μM was used for postmodification of NPTII@PICsomes. The efficiency of modifying PICsomes with KAibA was confirmed by RP-HPLC (Figure S2). The initial reaction mixture showed a peak assigned to N_3-KAibA at 24 min and a peak for alkyne-TEG-P(Lys-COOH) at 29 min. After the reaction, the chromatogram of the mixture showed a new peak at 27 min in addition to the peaks at 24 and 29 min. The new peak in HPLC was fractioned and confirmed as N_3-KAibA-conjugated alkyne-TEG-P(Lys-COOH) by MALDI-TOF-MS. The reaction efficiency was determined to be 42.3% by calculating the decrease in the area of the peak at 29 min. When 0.25 equiv of CPP against alkyne groups was reacted with PICsomes, the maximum reaction efficiency should be theoretically 25%; however, the reaction efficiency exceeded this value. This was explained by assuming that the actual concentration of alkyne-TEG-P(Lys-COOH) was low because the dissociated free peptide was removed by dialysis before the click reaction.

Finally, the capability of the PICsomes containing NPTII to internalize into plant cells was examined using seedlings of *A. thaliana*. Solutions of RhB-NPTII@KAibA-PICsomes or RhB-NPTII@PICsomes were infiltrated into the seedlings using the vacuum method.[15] After incubation for 24 h, these seedlings were observed by CLSM to confirm that RhB-NPTII was internalized into the plant cells (Figure 9). The cell wall was stained with calcofluor white. RhB-NPTII@KAibA-PICsomes were introduced into not the leaf cells but the root cells (Figure S3). Therefore, we focused on the root hairs of the seedlings for further investigation of PICsome internalization. In CLSM images of the seedlings infiltrated with RhB-NPTII@KAibA-PICsomes, the red fluorescence signal derived from RhB was observed inside the root hair cells of the seedlings. In contrast, in the case of RhB-NPTII@PICsomes, the fluorescence from RhB was faint, and all the signal merged with the signal of calcofluor white. These results indicate that the PICsomes modified with KAibA at the surface can penetrate the cell wall and membrane and that RhB-NPTII was then successfully internalized into the root cells.

PICsomes are expected to maintain the activity of the encapsulated enzyme for a long time in plants because the PICsomes can protect the encapsulated enzyme from innate proteases in plants. The time course of the CLSM images of the seedlings infiltrated with RhB-NPTII@KAibA-PICsomes or only RhB-NPTII was observed for evaluating the long-term

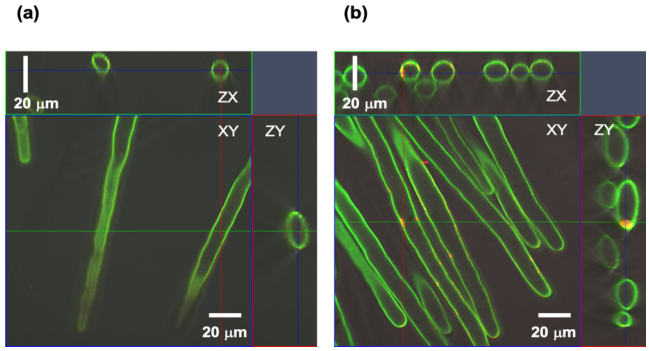

Figure 9. Z-stacked CLSM images of seedlings (*A. thaliana*) infiltrated with unmodified PICsomes (a) or KAibA-PICsomes (b) containing RhB-NPTII. The center image shows one picture from 40 z-stack images. The green-framed image represents the ZX plane on the green line. The red-framed image represents the ZY plane on the red line. Fluorescence from RhB-NPTII (red) was observed in the root hair cells stained with calcofluor white (green).

stability of RhB-NPTII encapsulated in KAibA-PICsomes in plant cells. The fluorescence of RhB-NPTII was observed in the root hair cells of seedlings up to 10 days after infiltration (Figure 10). In the absence of PICsomes, the fluorescence from RhB-NPTII disappeared within 2 days, indicating that NPTII was rapidly degraded by proteolysis in the plant cells (Figure S4). Therefore, PICsomes significantly improved the stability of NPTII in NPTII@KAibA-PICsomes by protecting it from proteases.

To confirm that NPTII@KAibA-PICsomes exhibit enzymatic activity in plant cells, we carried out selection of the seedlings in the presence of kanamycin. A solution of NPTII@KAibA-PICsomes was infiltrated into the seedlings of *A. thaliana*, and the seedlings were incubated on an agar medium containing kanamycin (10 mg L^{-1}). As a control experiment, solutions of NPTII or only Bis−Tris buffer were infiltrated into seedlings for selection using kanamycin. These seedlings were cultured on a kanamycin-containing medium covered with a plastic sheet with holes to implant the roots of seedlings (Figure S5). As shown in Figure 10, KAibA-PICsomes were introduced in root hair cells, and hence, we considered the activity of NPTII to be mostly exhibited in the root hair. After 1 week of incubation, as an indicator of plant growth, the dry weights of 14 seedlings were measured at once and replicated five times (Figure 11, Figure S6). The seedlings infiltrated with each solution exhibited similar dry weights when these seedlings were grown in the absence of kanamycin. From this result, it is inferred that there was no growth inhibition or growth promotion in the seedlings infiltrated with NPTII or PICsome solution. In the presence of 10 mg L^{-1} of kanamycin, the dry weights of seedlings infiltrated with NPTII or Bis−Tris buffer significantly decreased in comparison with those of seedlings grown in the absence of kanamycin (Figure S7). The dry weights of seedlings treated with NPTII were the same as those of the seedlings treated with Bis−Tris buffer. Therefore, kanamycin resistance was not expressed by the introduction of only NPTII. In contrast, the dry weights of seedlings infiltrated with NPTII@KAibA-PICsomes and grown in the presence of kanamycin were comparable to those of seedlings grown in the absence of kanamycin. In addition, the dry weights of seedlings infiltrated with the NPTII@KAibA-PICsome solution were significantly larger than those of seedlings infiltrated with NPTII or only Bis−Tris buffer. Based on these results,

https://dx.doi.org/10.1021/acs.biomac.0c01380
Biomacromolecules 2021, 22, 1080−1090

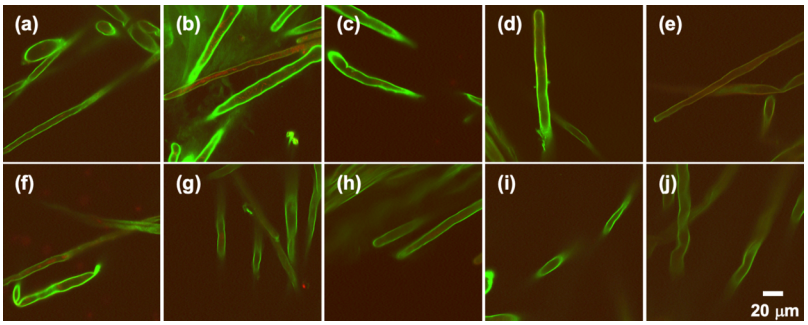

Figure 10. Time course of CLSM images of the seedlings infiltrated with RhB-NPTII@KAibA-PICsomes. These seedlings were observed at (a) 1, (b) 2, (c) 3, (d) 4, (e) 5, (f) 6, (g) 7, (h) 10, (i) 14, and (j) 18 days after treatment with the RhB-NPTII@KAibA-PICsome solution. Fluorescence from RhB (red) was observed in the root hair cells stained with calcofluor white (green) for up to 10 days.

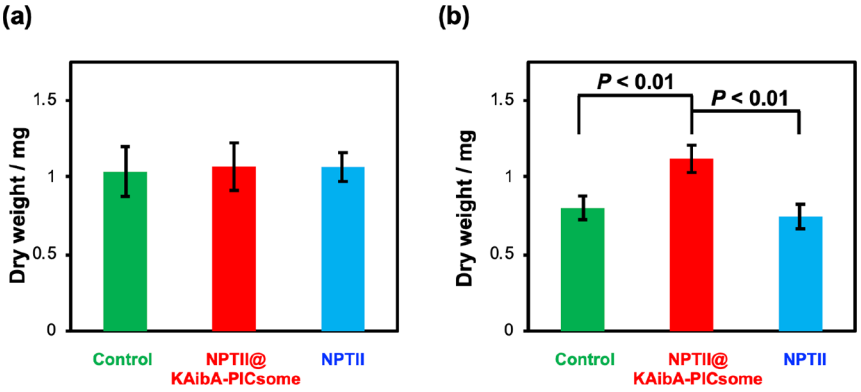

Figure 11. Dry weights of 14 seedlings grown in the absence (a) or presence (b) of kanamycin (10 mg L^{-1}) in 7 days after infiltration with Bis–Tris buffer, NPTII@KAibA-PICsomes, or only NPTII. Error bars represent the standard deviation from the mean (n = 5). The P value was determined based on the Mann–Whitney test, and a value of $P < 0.05$ was considered statistically significant.

kanamycin resistance was successfully imparted to the seedlings by the introduction of NPTII@KAibA-PICsomes.

CONCLUSIONS

In this study, we developed a novel PICsome consisting of polycationic and polyanionic peptides, P(Lys) and alkyne-TEG-P(Lys-COOH), which have an alkyne group at the terminus, that enabled enzyme delivery to add a trait to plants for a long period. Cross-sectional FESEM images showed that mixing P(Lys) and alkyne-TEG-P(Lys-COOH) and subsequent cross-linking resulted in hollow spheres, indicating the successful formation of PICsomes. The model protein NPTII was encapsulated into the PICsomes and maintained its enzymatic activity. Modifying the PICsomes with KAibA as a CPP resulted in PICsomes that delivered NPTII into the root hair cells of seedlings and protected it from proteases for a long period (up to 10 days). The seedlings treated with KAibA-PICsomes containing NPTII exhibited kanamycin resistance. This PICsome can be modified with various peptides bearing N_3 groups. Therefore, in the future, if an organelle translocation sequence needs to be modified, a protein can be selectively introduced into that organelle. This assembly is expected to be a useful protein carrier.

ASSOCIATED CONTENT

Supporting Information

The Supporting Information is available free of charge at https://pubs.acs.org/doi/10.1021/acs.biomac.0c01380.

FESEM image of KAibA-modified PICsomes; CLSM image of seedlings treated with RhB-NPTII@KAibA-PICsomes; time course of CLSM images of root hair of seedlings treated with RhB-NPTII only; images and dry weights of seedlings grown in the absence or presence of kanamycin (10 mg L^{-1}) after 7 days (PDF).

AUTHOR INFORMATION

Corresponding Authors

Kousuke Tsuchiya − *Department of Material Chemistry, Graduate School of Engineering, Kyoto University, Kyoto 615-8510, Japan;* orcid.org/0000-0003-2364-8275; Email: tsuchiya.kosuke.3n@kyoto-u.ac.jp

Keiji Numata − *Department of Material Chemistry, Graduate School of Engineering, Kyoto University, Kyoto 615-8510, Japan; Biomacromolecules Research Team, RIKEN Center for Sustainable Resource Science, Saitama 351-0198, Japan;* orcid.org/0000-0003-2199-7420; Email: numata.keiji.3n@kyoto-u.ac.jp

Authors

Seiya Fujita − *Department of Material Chemistry, Graduate School of Engineering, Kyoto University, Kyoto 615-8510, Japan*

Yoko Motoda − *Biomacromolecules Research Team, RIKEN Center for Sustainable Resource Science, Saitama 351-0198, Japan*

Takanori Kigawa − *RIKEN Center for Biosystems Dynamics Research, Laboratory for Cellular Structural Biology,*

https://dx.doi.org/10.1021/acs.biomac.0c01380
Biomacromolecules 2021, 22, 1080−1090

Yokohama, Kanagawa 230-0045, Japan; orcid.org/0000-0003-0146-9719

Complete contact information is available at: https://pubs.acs.org/10.1021/acs.biomac.0c01380

Author Contributions

K.T. and K.N. conceived and designed the research. S.F. performed all the experiments, analyzed the data, and wrote the manuscript. T. K. and Y.M. synthesized the enzymes. All authors reviewed the manuscript.

Notes

The authors declare no competing financial interest.

■ ACKNOWLEDGMENTS

This work was supported by JST ERATO Grant No. JPMJER1602, Japan (K.N.), L-INSIGHT fellowship program of Kyoto University (K.N.), and JSPS KAKENHI Grant No. JP19K15643 (S.F.).

■ REFERENCES

(1) Krishna, G.; Singh, B. K.; Kim, E. K.; Morya, V. K.; Ramteke, P. W. Progress in Genetic Engineering of Peanut (Arachis Hypogaea L.)-A Review. *Plant Biotechnol. J.* **2015**, *13*, 147−162.

(2) Ali, F.; Bano, A.; Fazal, A. Recent Methods of Drought Stress Tolerance in Plants. *Plant Growth Regul.* **2017**, *82*, 363−375.

(3) Nadeem, M.; Li, J.; Yahya, M.; Wang, M.; Ali, A.; Cheng, A.; Wang, X.; Ma, C. Grain Legumes and Fear of Salt Stress: Focus on Mechanisms and Management Strategies. *Int. J. Mol. Sci.* **2019**, *20*, 799.

(4) Ackova, D. G. Heavy metals and their general toxicity for plants. *Plant Sci. Today* **2018**, *5*, 14−18.

(5) Kumar, K.; Gambhir, G.; Dass, A.; Tripathi, A. K.; Singh, A.; Jha, A. K.; Yadava, P.; Choudhary, M.; Rakshit, S. Genetically Modified Crops: Current Status and Future Prospects. *Planta* **2020**, *251*, 1−27.

(6) Jansing, J.; Schiermeyer, A.; Schillberg, S.; Fischer, R.; Bortesi, L. Genome Editing in Agriculture: Technical and Practical Considerations. *Int. J. Mol. Sci.* **2019**, *20*, 2888.

(7) Demirer, G. S.; Landry, M. P. Delivering Genes to Plants. *Chem. Eng. Prog.* **2017**, *113*, 40−45.

(8) Prakash, D.; Verma, S.; Bhatia, R.; Tiwary, B. N. Risks and Precautions of Genetically Modified Organisms. *ISRN Ecol.* **2011**, *2011*, 1−13.

(9) Bilichak, A.; Sastry-Dent, L.; Sriram, S.; Simpson, M.; Samuel, P.; Webb, S.; Jiang, F.; Eudes, F. Genome Editing in Wheat Microspores and Haploid Embryos Mediated by Delivery of ZFN Proteins and Cell-Penetrating Peptide Complexes. *Plant Biotechnol. J.* **2020**, *18*, 1307−1316.

(10) Thagun, C.; Motoda, Y.; Kigawa, T.; Kodama, Y.; Numata, K. Simultaneous Introduction of Multiple Biomacromolecules into Plant Cells Using a Cell-Penetrating Peptide Nanocarrier. *Nanoscale* **2020**, *12*, 18844−18856.

(11) Thagun, C.; Chuah, J. A.; Numata, K. Targeted Gene Delivery into Various Plastids Mediated by Clustered Cell-Penetrating and Chloroplast-Targeting Peptides. *Adv. Sci.* **2019**, *6*, 1902064.

(12) Guo, B.; Itami, J.; Oikawa, K.; Motoda, Y.; Kigawa, T.; Numata, K. Native Protein Delivery into Rice Callus Using Ionic Complexes of Protein and Cell-Penetrating Peptides. *PLoS One* **2019**, *14*, No. e0214033.

(13) Miyamoto, T.; Tsuchiya, K.; Numata, K. Block Copolymer/Plasmid DNA Micelles Postmodified with Functional Peptides via Thiol-Maleimide Conjugation for Efficient Gene Delivery into Plants. *Biomacromolecules* **2019**, *20*, 653−661.

(14) Midorikawa, K.; Kodama, Y.; Numata, K. Vacuum/Compression Infiltration-Mediated Permeation Pathway of a Peptide-PDNA Complex as a Non-Viral Carrier for Gene Delivery in Planta. *Sci. Rep.* **2019**, *9*, 1−10.

(15) Kang, Z.; Ding, G.; Meng, Z.; Meng, Q. The Rational Design of Cell-Penetrating Peptides for Application in Delivery Systems. *Peptides* **2019**, *121*, 170149.

(16) Xu, J.; Khan, A. R.; Fu, M.; Wang, R.; Ji, J.; Zhai, G. Cell-Penetrating Peptide: A Means of Breaking through the Physiological Barriers of Different Tissues and Organs. *J. Controlled Release* **2019**, *309*, 106−124.

(17) Ruseska, I.; Zimmer, A. Internalization Mechanisms of Cell-Penetrating Peptides. *Beilstein J. Nanotechnol.* **2020**, *11*, 101−123.

(18) Numata, K.; Horii, Y.; Oikawa, K.; Miyagi, Y.; Demura, T.; Ohtani, M. Library Screening of Cell-Penetrating Peptide for BY-2 Cells, Leaves of Arabidopsis, Tobacco, Tomato, Poplar, and Rice Callus. *Sci. Rep.* **2018**, *8*, 1−17.

(19) Ng, K. K.; Motoda, Y.; Watanabe, S.; Othman, A. S.; Kigawa, T.; Kodama, Y.; Numata, K. Intracellular Delivery of Proteins via Fusion Peptides in Intact Plants. *PLoS One* **2016**, *11*, 1−19.

(20) Numata, K.; Horii, Y.; Motoda, Y.; Hirai, N.; Nishitani, C.; Watanabe, S.; Kigawa, T.; Kodama, Y. Direct Introduction of Neomycin Phosphotransferase II Protein into Apple Leaves to Confer Kanamycin Resistance. *Plant Biotechnol.* **2016**, *33*, 403−407.

(21) Klermund, L.; Castiglione, K. Polymersomes as Nanoreactors for Preparative Biocatalytic Applications: Current Challenges and Future Perspectives. *Bioprocess Biosyst. Eng.* **2018**, *41*, 1233−1246.

(22) Rideau, E.; Dimova, R.; Schwille, P.; Wurm, F. R.; Landfester, K. Liposomes and Polymersomes: A Comparative Review towards Cell Mimicking. *Chem. Soc. Rev.* **2018**, *47*, 8572−8610.

(23) Jones, S. J.; Taylor, A. F.; Beales, P. A. Towards Feedback-Controlled Nanomedicines for Smart, Adaptive Delivery. *Exp. Biol. Med.* **2019**, *244*, 283−293.

(24) Leong, J.; Teo, J. Y.; Aakalu, V. K.; Yang, Y. Y.; Kong, H. Engineering Polymersomes for Diagnostics and Therapy. *Adv. Healthcare Mater.* **2018**, *7*, 1−27.

(25) Pandey, B.; Mahato, J.; Cotta, K. B.; Das, S.; Sharma, D. K.; Gupta, S. S.; Chowdhury, A. Glycopolypeptide-Grafted Bioactive Polyionic Complex Vesicles (PICsomes) and Their Specific Polyvalent Interactions. *ACS Omega* **2016**, *1*, 600−612.

(26) Li, J.; Liang, L.; Liang, J.; Wu, W.; Zhou, H.; Guo, J. Constructing Asymmetric Polyion Complex Vesicles via Template Assembling Strategy: Formulation Control and Tunable Permeability. *Nanomaterials* **2017**, *7*, 387.

(27) Nakai, K.; Ishihara, K.; Kappl, M.; Fujii, S.; Nakamura, Y.; Yusa, S. i. Polyion Complex Vesicles with Solvated Phosphobetaine Shells Formed from Oppositely Charged Diblock Copolymers. *Polymer* **2017**, *9*, 49.

(28) Ohara, Y.; Nakai, K.; Ahmed, S.; Matsumura, K.; Ishihara, K.; Yusa, S. I. PH-Responsive Polyion Complex Vesicle with Polyphosphobetaine Shells. *Langmuir* **2018**, *35*, 1249−1256.

(29) Wang, X.; Yao, C.; Zhang, G.; Liu, S. Regulating Vesicle Bilayer Permeability and Selectivity via Stimuli-Triggered Polymersome-to-PICsome Transition. *Nat. Commun.* **2020**, *11*, 1−13.

(30) Anraku, Y.; Kishimura, A.; Oba, M.; Yamasaki, Y.; Kataoka, K. Spontaneous Formation of Nanosized Unilamellar Polyion Complex Vesicles with Tunable Size and Properties. *J. Am. Chem. Soc.* **2010**, *132*, 1631−1636.

(31) Koide, A.; Kishimura, A.; Osada, K.; Jang, W. D.; Yamasaki, Y.; Kataoka, K. Semipermeable Polymer Vesicle (PICsome) Self-Assembled in Aqueous Medium from a Pair of Oppositely Charged Block Copolymers: Physiologically Stable Micro-/Nanocontainers of Water-Soluble Macromolecules. *J. Am. Chem. Soc.* **2006**, *128*, 5988−5989.

(32) Kishimura, A.; Koide, A.; Osada, K.; Yamasaki, Y.; Kataoka, K. Encapsulation of Myoglobin in PEGylated Polyion Complex Vesicles Made from a Pair of Oppositely Charged Block Ionomers: A Physiologically Available Oxygen Carrier. *Angew. Chem., Int. Ed.* **2007**, *46*, 6085−6088.

(33) Li, J.; Anraku, Y.; Kataoka, K. Self-Boosting Catalytic Nanoreactors Integrated with Triggerable Crosslinking Membrane Networks for Initiation of Immunogenic Cell Death by Pyroptosis. *Angew. Chem., Int. Ed.* **2020**, *59*, 13526−13530.

(34) Anraku, Y.; Kishimura, A.; Kamiya, M.; Tanaka, S.; Nomoto, T.; Toh, K.; Matsumoto, Y.; Fukushima, S.; Sueyoshi, D.; Kano, M. R.; Urano, Y.; Nishiyama, N.; Kataoka, K. Systemically Injectable Enzyme-Loaded Polyion Complex Vesicles as in Vivo Nanoreactors Functioning in Tumors. *Angew. Chem., Int. Ed.* **2016**, *55*, 560−565.
(35) Numata, K.; Baker, P. J. Synthesis of Adhesive Peptides Similar to Those Found in Blue Mussel (Mytilus Edulis) Using Papain and Tyrosinase. *Biomacromolecules* **2014**, *15*, 3206−3212.
(36) Tsuchiya, K.; Kurokawa, N.; Gimenez-Dejoz, J.; Gudeangadi, P. G.; Masunaga, H.; Numata, K. Periodic Introduction of Aromatic Units in Polypeptides via Chemoenzymatic Polymerization to Yield Specific Secondary Structures with High Thermal Stability. *Polym. J.* **2019**, *51*, 1287−1298.
(37) Chen, J.; Miller, A.; Kirchmaier, A. L.; Irudayaraj, J. M. K. Single-Molecule Tools Elucidate H2A.Z Nucleosome Composition. *J. Cell Sci.* **2012**, *125*, 2954−2964.
(38) Tsuchiya, K.; Numata, K. Papain-Catalyzed Chemoenzymatic Synthesis of Telechelic Polypeptides Using Bis(Leucine Ethyl Ester) Initiator. *Macromol. Biosci.* **2016**, 1001−1008.
(39) Schwab, L. W.; Kloosterman, W. M. J.; Konieczny, J.; Loos, K. Papain Catalyzed (Co)Oligomerization of α-Amino Acids. *Polymer* **2012**, *4*, 710−740.
(40) Qin, X.; Xie, W.; Tian, S.; Ali, M. A.; Shirke, A.; Gross, R. A. Influence of Nε-Protecting Groups on the Protease-Catalyzed Oligomerization of L-Lysine Methyl Ester. *ACS Catal.* **2014**, *4*, 1783−1792.
(41) Tsuchiya, K.; Numata, K. Chemoenzymatic Synthesis of Polypeptides for Use as Functional and Structural Materials. *Macromol. Biosci.* **2017**, *17*, 1700177.
(42) Chuanoi, S.; Kishimura, A.; Dong, W. F.; Anraku, Y.; Yamasaki, Y.; Kataoka, K. Structural Factors Directing Nanosized Polyion Complex Vesicles (Nano-PICsomes) to Form a Pair of Block Aniomer/Homo Catiomers: Studies on the Aniomer Segment Length and the Catiomer Side-Chain Structure. *Polym. J.* **2014**, *46*, 130−135.
(43) Yilmaz, N.; Kodama, Y.; Numata, K. Revealing the Architecture of the Cell Wall in Living Plant Cells by Bioimaging and Enzymatic Degradation. *Biomacromolecules* **2020**, *21*, 95−103.
(44) Hori, M.; Cabral, H.; Toh, K.; Kishimura, A.; Kataoka, K. Robust Polyion Complex Vesicles (PICsomes) under Physiological Conditions Reinforced by Multiple Hydrogen Bond Formation Derived by Guanidinium Groups. *Biomacromolecules* **2018**, *19*, 4113−4121.
(45) Lakshmanan, M.; Kodama, Y.; Yoshizumi, T.; Sudesh, K.; Numata, K. Rapid and Efficient Gene Delivery into Plant Cells Using Designed Peptide Carriers. *Biomacromolecules* **2012**, *14*, 10−16.
(46) Terada, K.; Gimenez-Dejoz, J.; Miyagi, Y.; Oikawa, K.; Tsuchiya, K.; Numata, K. Artificial Cell-Penetrating Peptide Containing Periodic α-Aminoisobutyric Acid with Long-Term Internalization Efficiency in Human and Plant Cells. *ACS Biomater. Sci. Eng.* **2020**, *6*, 3287−3298.

https://dx.doi.org/10.1021/acs.biomac.0c01380
Biomacromolecules 2021, 22, 1080−1090